Synthesis and Self-Assembly of Pseudo-Spherical Homo- and Heterodimeric Capsules

Carlos Valdés, Urs P. Spitz, Leticia M. Toledo, Stefan W. Kubik, and Julius Rebek, Jr.*

Contribution from the Department of Chemistry, Massachusetts Institute of Technology, Cambridge, Massachusetts 02139

Received June 9, 1995. Revised Manuscript Received October 25, 1995[⊗]

Abstract: Experimental details are given for the synthesis and characterization of several new molecules capable of self-assembly. The new molecules feature glycoluril subunits held apart by various rigid spacers, ethylene (**2**), naphthalene (**3**), and ethenoanthracene (**4**), and assemble through hydrogen bonds into pseudo-spherical dimeric capsules. The nature of their assembly is demonstrated by the X-ray crystal structure of capsules **1·1**. The capsules are shown to enclose smaller guest molecules in a reversible manner. Direct evidence of the guest molecules inside the capsules from NMR is presented. In addition to self-assembling dimerically, these new molecules are shown to disproportionate into hybrid species or heterodimers. The resulting new capsules feature internal cavities of varying sizes and shapes. Formation of hybrid dimers **1·2**, **1·4**, and **3·4** is observed in solutions containing mixtures of two homodimers. The disproportionation equilibria could be manipulated by the addition of appropriately sized solvents as guests. Even the energetically unlikely hybrids **1·4** and **3·4** are found to be the dominant species when suitable guests such as $CDBr_3$ are present. Evidence of the existence of the heterodimers is presented from NOE measurements. Factors controlling the heterodimerization are discussed.

Introduction

Assemblies of small molecules provide a means for exploring the intermolecular forces involved in molecular recognition and the chemical information that becomes expressed when superstructures emerge. In addition, small molecular assemblies can provide models for the macromolecular assemblies involved in a large number of biological processes. A minimalist model for some of these processes has been found in structure **1**, which self-assembles in organic solvents to **1·1**, a dimer of roughly

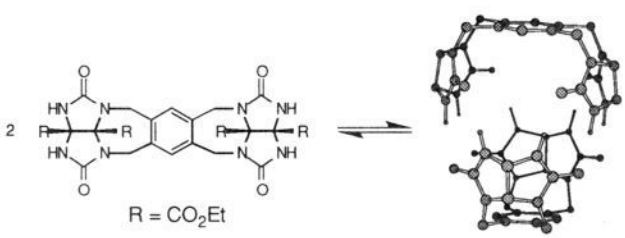

1 1·1

spherical shape.[1] The dimeric form is held together by a seam of eight hydrogen bonds. The glycoluril functions at the ends of the molecule present an array of hydrogen bond donor and acceptor sites that is self-complementary, and the stereochemical features impart a curvature to the structure that encourages dimerization.[2,3] The cavity of the dimer can function as a host for guests of complementary size and shape.[4,5]

Here we report the crystal structure of the **1·1** dimer and a number of structural variations on the basic skeleton of **1**. X-ray crystallography revealed that in the solid state compound **1** indeed exists as the semispherical **1·1** dimer. The geometry of the dimer and its hydrogen bonds are in high agreement with the previously proposed structure from solution NMR and MacroModel modeling studies.

In molecules **2**, **3**, and **4**, all variations on **1**, the glycoluril functions at the end of the molecule and the molecular recognition elements they encode remain constant. The connecting spacer elements, which provide the information on the size and the overall shape of the dimer, are varied. The analogs prepared lead to unusual pseudo-spherical structures with cavities smaller or larger than that of **1·1**. In addition, *heterodimers* were observed in experiments using two different dimers in the same solution. The resulting hybrid capsules showed that structurally related molecules that are self-complementary can also show complementarity to each other. We found that the recombinations or disproportionations of the dimers can be manipulated by the addition of suitably sized guests, a phenomenon related to *nucleation*.

[⊗] Abstract published in *Advance ACS Abstracts,* December 1, 1995.

(1) For 3-dimensional supramolecular aggregates, see: (a) Seto, C.; Whitesides, G. M. *J. Am. Chem. Soc.* **1991**, *113*, 712−713. (b) Simard, M.; Su, D.; Wuest, J. D. *J. Am. Chem. Soc.* **1991**, *113*, 4696−4698. (c) Baxter, P.; Lehn, J.-M.; DeCian, A.; Fischer, J. *Angew.Chem., Int. Ed. Engl.* **1993**, *32*, 69−72. (d) Bonar-Law, R. P.: Sanders, J. K. M. *Tetrahedron Lett.* **1993**, *34*, 1677−1680. (e) Ghadiri, M. R.; Granja, J. R.; Milligan, R. A.; McRee, D. E.; Khazanovich, N. *Nature* **1993**, *366*, 324−327. (f) Yang, J.; Fan, E.; Geib, S.; Hamilton, A. D. *J. Am. Chem. Soc.* **1993**, *115*, 5314−5315. (g) Ghadiri, M. R.; Granja, J. R.; Buehler, L. K. *Nature* **1994**, *369*, 133−137. (h) Mathias, J. P.; Seto, C. T.; Simanek, E. E.; Whitesides, G. M. *J. Am. Chem. Soc.* **1994**, *116*, 1725−1736. (i) Mathias, J. P.; Simanek, E. E.; Zerkowski, J. A.; Seto, C. T.; Whitesides, G. M. *J. Am. Chem. Soc.* **1994**, *116*, 4316−4325. (j) Mathias, J. P.; Simanek, E. E.; Whitesides, G. M. *J. Am. Chem. Soc.* **1994**, *116*, 4326−4340.

(2) Wyler, R.; de Mendoza, J.; Rebek, J., Jr. *Angew. Chem., Int. Ed. Engl.* **1993**, *32*, 1699−1701.

(3) A very recent example of hydrogen-bond-driven dimerization of a self-complementary tridimensional structure. (a) Ghadiri, M. R.; Kobayashi, K.; Granja, J. R.; Chadha, R. K.; McRee, D. E. *Angew.Chem., Int. Ed. Engl.* **1995**, *34*, 93. (b) *Ibid.* **1995**, *34*, 95.

(4) (a) Branda, N.; Wyler, R.; Rebek, J., Jr. *Science* **1994**, *263*, 1267−1268. (b) Branda, N.; Grotzfeld, R. M.; Valdés, C.; Rebek, J., Jr. *J. Am. Chem. Soc.* **1995**, *117*, 85−88.

(5) For previous examples of encapsulation of neutral molecules, see: (a) Cram, D. J. *Nature* **1992**, 29. (b) Cram, D. J.; Jaeger, R.; Deshayes, K. *J. Am. Chem. Soc.* **1993**, *115*, 10111. (c) Eid, C. N., Jr.; Knobler, C. B.; Gronbeck, D. A.; Cram, D. J. *J. Am. Chem. Soc.* **1994**, *116*, 8506. (d) Collet, A. *Tetrahedron* **1987**, *43*, 5725. (d) Hatt, R. M.; Bradshaw, J. S.; Pawlak, K.; Bruening, R. L.; Tarbet, B. J. *Chem. Rev.* **1992**, *92*, 1261. (e) Timmermann, P.; Verboom, W.; van Veggel, F. C. J. M.; van Duynhoven, J. P. M.; Reinhoudt, D. N. *Angew. Chem., Int. Ed. Engl.* **1994**, *33*, 2345.

0002-7863/95/1517-12733$09.00/0

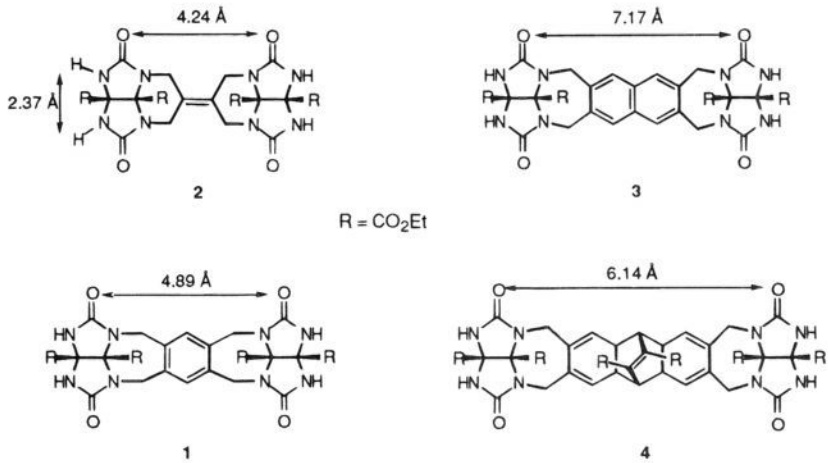

Figure 1. Dimensions of monomers **1**−**4** obtained from MM2 calculations.

Table 1. Energy-Minimized Structures of Dimers of **2**, **3** and **4**

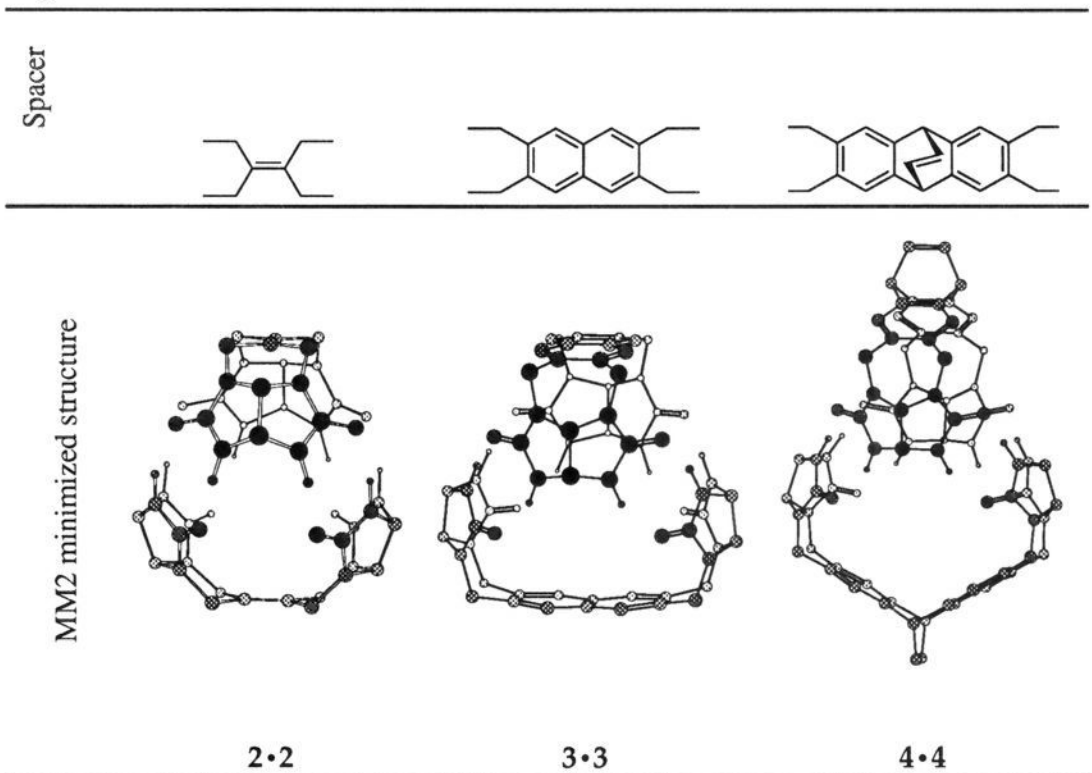

The new monomers **2**, **3**, and **4** contain ethylene, naphthalene, and a bridged anthracene, respectively, as their spacer elements. The energy-minimized structures of the corresponding dimers, as generated by an MM2 forcefield,[6] are provided in Table 1, and the dimensions of the monomers (also from MM2 minimization) are shown in Figure 1. In the homodimeric assemblies, the two halves are mirror images rotated by 90° relative to each other (S_4 symmetry). Thus, if good hydrogen bonds are to be formed in the dimers, the "length" of the spacer should roughly correspond to the "width" of the glycoluril (Figure 1), and the O−O distances shown must complement the H−H distances on the glycoluril. The H−H distances on the glycoluril are fixed, but the O−O distances are a function of the spacer's size and shape.

We compared the MM2-minimized dimers of **2**, **3**, and **4** with **1·1** to predict the likelihood of dimerization for the new molecules. For instance, the small difference in O−O distances between the ethylene spacer in **2** and the benzene spacer in **1** (~0.6 Å) could be compensated by a flattening in **2** of the two rings connecting the ethylene spacer and the glycolurils. The obstacles to self-assembly of naphthalene derivative **3** appear more challenging. The increase in O−O distances is >2 Å. If all eight possible hydrogen bonds were to form in **3·3,** the π-surface of the naphthalene would have to bend and little driving force for dimerization would be expected (Figure 1, Table 1). The bridged anthracene spacer of **4** appears at first glance to separate the glycolurils even further, but the ethylene bridge provides a crease in the middle of the skeleton that could correct for the oversized nature of the spacer (Figure 1, Table 1). Here, the glycoluril hydrogens are directed somewhat inward, a feature that leads to dimeric structure **4·4**, whose halves are connected along a narrower seam. According to our

(6) Molecular Modeling was performed using MacroModel 3.5X (MM2* force field). Mohamadi, F.; Richards, N. G.; Guida, W. C.; Liskamp, R.; Lipton, M.; Caufield, C.; Chang, G.; Hendrickson, T.; Still, W. C. *J. Comput. Chem.* **1990**, *11*, 440−467.

Scheme 1

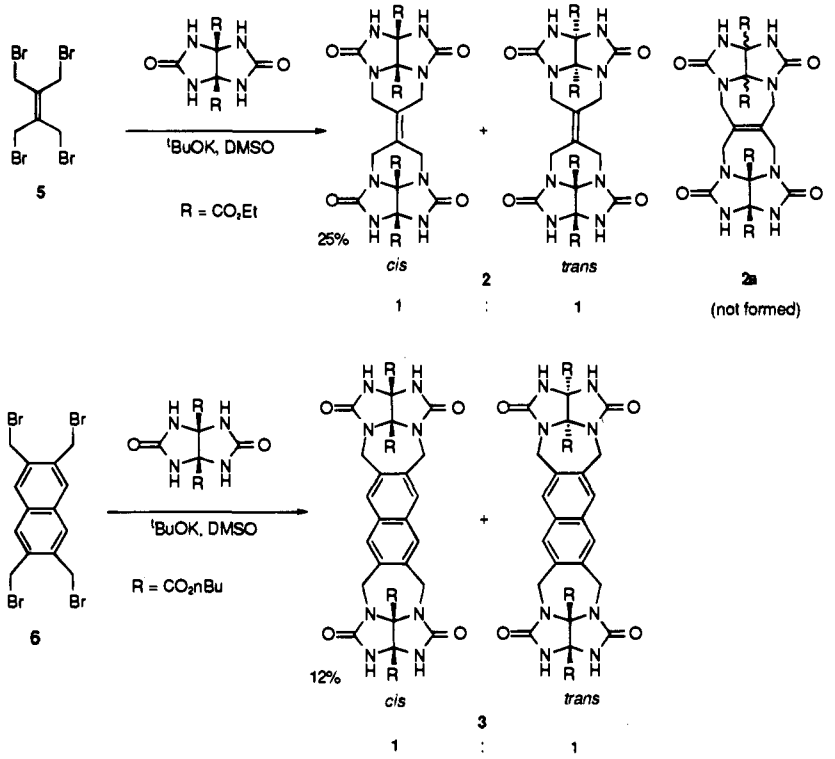

modeling studies, structure **4** could dimerize to create a cavity much larger than that of **1**·**1**.[7]

Synthesis

Analogs **2** and **3** were synthesized by treatment of the corresponding tetrabromides (**5** or **6**) with large excess of the glycoluril in DMSO/^{t}BuOK.[4b] The coupling proceeded uneventfully to give mixtures of two isomers in an approximately 1:1 ratio (Scheme 1). The cis isomers are generally much more soluble in nonpolar solvents than the trans isomers, and **2** and **3** were readily isolated by extraction with chloroform. X-ray crystallography has confirmed that the coupling reaction of **5**[8] with glycoluril derivatives gives structure **2**, rather than **2a**.[9]

Tetrakis(bromomethyl)naphthalene derivative **6** was obtained from tetramethyl naphthalene-2,3,6,7-tetracarboxylate.[10] Reduction of the esters and acetylation of the tetra-alcohol, followed by bromination with HBr in acetic acid, gave the desired tetrabromide in high yield (Scheme 2).

For spectroscopic comparisons of assemblies to aggregates of mere nonspecific association, two reference compounds **8** and **9** were prepared. These bear the same hydrogen-bonding

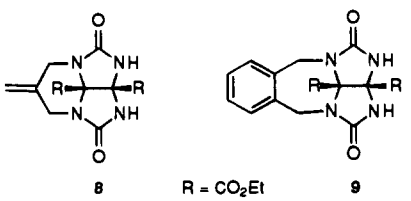

sites but lack the features required for a specific dimeric assembly. They were obtained by alkylation of the glycoluril by the appropriate dichloro precursors.

Scheme 2

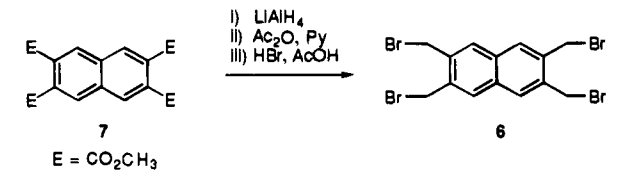

Scheme 3

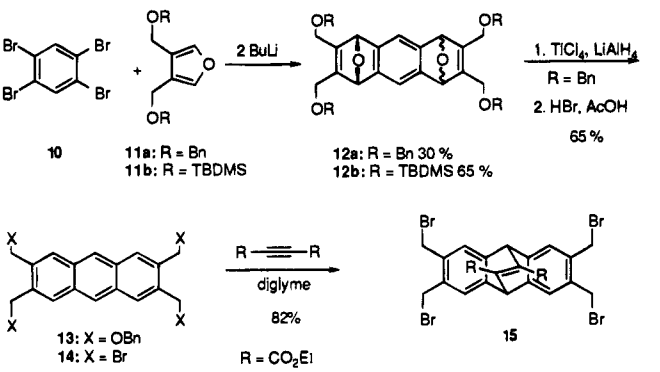

Similarly, the synthesis of **4** was accomplished by coupling two glycolurils with the bridged anthracene spacer **15**. The key step in the synthesis of **15** (Scheme 3) involved the reaction of 1,2,4,5-tetrabromobenzene (**10**) with 2.2 equiv of BuLi in the presence of excess 3,4-disubstituted furan **11**. Tandem benzyne cycloadditions to furans of this kind were introduced by Hart.[11] For the case at hand, the cycloadditions gave mixtures of two isomeric endoxides, *syn* and *anti* **12**, in 30% (R = Bn) or 65% (R = TBDMS) combined yield. The tetrasubstituted anthracene **13** was obtained from **12a** by Ti(0) reduction[12] of the *syn/anti* mixture. Treatment of the tetrabenzyl ether with HBr/AcOH

(7) Valdés, C.; Spitz, U. P.; Kubik, S. W.; Rebek, J., Jr. *Angew. Chem., Int. Ed. Engl.* **1995**, *34*, 1885.

(8) Le Quesne, P. W.; Reynolds, M. A.; Beda, S. E.; *J. Org. Chem.* **1975**, *40*, 142.

(9) Supporting this interpretation, a disordered guest was also found in the crystal of **2**·**2**, the X-ray structure of which has recently been determined and will be reported in due course.

(10) Thomas, A. D.; Miller, L. L. *J. Org. Chem.* **1986**, *51*, 4160.

(11) Hart, H.; Lay, C.; Nwokogu, G. C.; Shamouilian, S. *Tetrahedron* **1987**, *43*, 5203.

(12) Huang, N. Z.; Xing, Y. D.; Ye, D. Y. *Synthesis* **1982**, 1041−1044.

Scheme 4

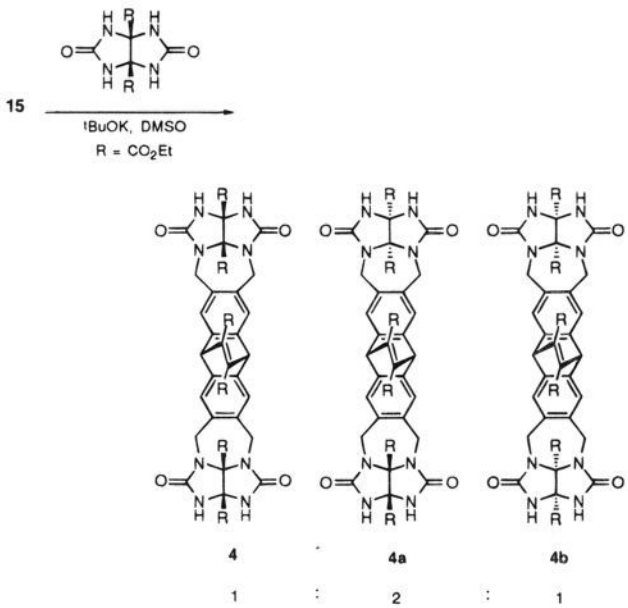

Table 2. Crystallographic Parameters for Compound **1**

a (Å)	13.924(3)
b (Å)	15.314(3)
c (Å)	18.094(4)
α (deg)	92.09(3)
β (deg)	98.65(3)
γ (deg)	117.24(3)
volume (Å^3)	3366(8)
space group,	$P\bar{1}$
Z	4
ρ_{calcd} (g/cm^3)	1.41
μ (cm^{-1})	1.11
radiation (λ) (Å)	Mo Kα (0.710 690)
2θ limit (deg)	46
temperature (°C)	−66
total/unique reflections	12856/8853
no. of observations ($I > 3\sigma$)	5716
no. of parameters	914
R	0.075
R_w	0.074

solution in chloroform yielded the tetrabromide **14** in 65% yield. Diels−Alder reaction of anthracene **14** with diethyl acetylenedicarboxylate proceeded at 160 °C in diglyme to give the desired ethenoanthracene tetrabromide **15** in excellent yield (Scheme 3).

Unlike in the preparation of **1**, **2**, or **3**, where two geometrical isomers are possible, the reaction of **15** with glycoluril[4b] gives a mixture of three isomers (Scheme 4). These were obtained in the expected statistical ratio (1:2:1); however, the enhanced solubility of the desired compound in nonpolar solvents allowed for its isolation by extraction with chloroform.[13] After purification by flash chromatography, target compound **4** was obtained in 12% yield.

Characterization

X-ray crystallographic analysis (Table 2, Figure 2) of a single crystal of **1**, obtained by slow evaporation from an 8:2 CH_2Cl_2:CH_3OH solution, confirmed its dimeric structure in the solid state. The structure of dimer **1·1** indeed resembles a semispherical capsule; eight almost linear hydrogen bonds (167−178°), in the range of 2.78−2.89 Å, hold the monomers together. The phenyl spacers and all four methylene groups connecting

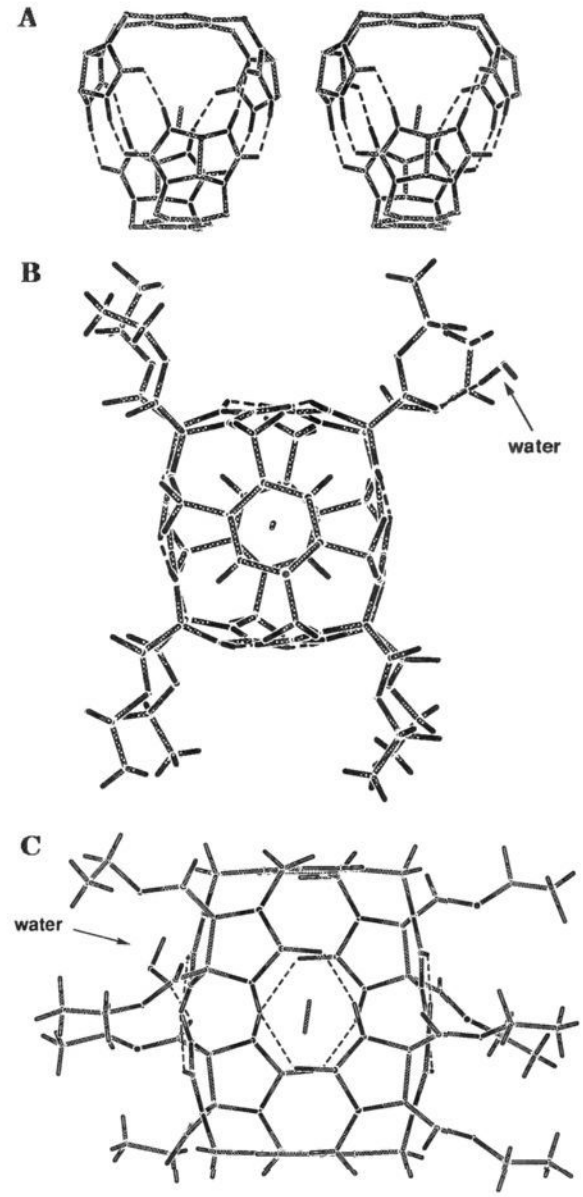

Figure 2. (A) Stereoview of capsule **1·1** obtained from crystallographic analysis. Ethyl ester groups have been omitted for clarity. (B and C) Two views highlighting hydrogen bond geometry and ester interactions.

the glycolurils are coplanar, imparting an almost tetrahedral geometry to the dimer. Interestingly, the potential S_4 symmetry of the dimer is lost since it crystallizes as two crystallographically unique molecules per asymmetric unit within triclinic space group $P\bar{1}$; the unit cell contains two dimers related by an inversion center.

The crystal of **1·1** appears to contain a disordered guest species in its cavity, although it was not possible to determine unambiguously the identity of the guest.[9] It was possible, however, to locate and refine a carbon atom at two positions with assigned occupancy factors of 0.55 and 0.45. This leads us to believe that this guest species is a methanol molecule with a highly disordered oxygen atom. Other work in this group has indicated that guests which can form hydrogen bonds to the atoms of the inside surface are readily encapsulated.[14] There are eight (carbonyl oxygen) potentially good hydrogen bond

(13) Among the three isomers, only **4** possesses a geometry that allows the formation of a discrete aggregate (dimer) via hydrogen bonds.

(14) Meissner, R. S.; Rebek, J., Jr.; de Mendoza, J. *Science* **1995**, *270*, 1485. Autoencapsulation Through Intermolecular Forces: A Synthetic Self-Assembling Spherical Complex.

acceptors along the seam of the capsule, and thus, it is possible that the oxygen atom of methanol may be disordered about eight positions.

The overall packing in the crystal structure is such that the hydrophobic ethyl ester groups on the convex sides of the glycolurils act as shields of the hydrophilic seam. The ester groups of vicinal dimers intercalate, thus maximizing packing efficiency and hydrophobic interactions. Also, there is a water molecule forming a hydrogen bond to one of the ester carbonyls. This causes a reversal of the orientation of this carbonyl with respect to the other seven ester carbonyls.

Table 3. ^{1}H NMR Chemical Shifts of Glycoluril Protons in Different Solvents

	chemical shift δ for the NH resonance (ppm)			IR NH (cm^{-1})[a]
	CD_2Cl_2	$CDCl_3$	$CDCl_2CDCl_2$	$CHCl_3$
1	8.50	9.13	9.02	3210
2	9.05	9.12	8.97	3217
3	8.28	7.83	7.26	3223, 3436
4	8.21	8.45	7.75	3229
8 (10 mM)	5.80	5.83	5.70	3442
9 (10 mM)	6.00	6.00	5.80	3442

[a] IR spectra were taken from 2 mM solutions.

The FT-IR spectra of a solution of **1** in $CHCl_3$ showed a single broad band around 3220 cm^{-1}, a characteristic feature of extensive hydrogen bonding. IR spectra of solutions of **2** and **4** in $CHCl_3$ showed identical absorbances, hinting that they may also form dimers as predicted by MM2 modeling. In contrast, the reference compounds **8** and **9**, at the same concentration, lacked this absorption at 3220 cm^{-1}. Sharp bands at 3442 cm^{-1}, which are characteristic for non-hydrogen-bonded N−H stretching of amides, were observed instead (Table 3). The IR spectrum of the naphthalene derivative **3** is particularly revealing. For this compound, a broad band at 3223 and a sharp band at 3436 cm^{-1} indicated the presence of both free and hydrogen-bonded amides. This is in agreement with the modeling study; since the naphthalene spacer of **3** is too long, only four hydrogen bonds can be formed at any given time in the **3·3** dimer. This leaves four NH groups relatively free (Table 1).

The ^{1}H NMR resonances of the glycoluril N-H protons in compounds **1**, **2**, and **4** in $CDCl_3$ (Table 3) appeared well within the range (>8 ppm) of hydrogen-bonded amides. Substantial downfield shifts were observed when compared to the corresponding resonances of **8** and **9** (<6 ppm), The corresponding chemical shift seen for **3·3** (7.83 ppm) suggests that it is formed as a partially hydrogen bonded dimer. This is consistent with the IR spectrum which clearly showed the presence of hydrogen-bonded and nonbonded NH groups (*vide supra*). On the NMR time scale, an average resonance is observed and **3·3** appears to have eight mediocre hydrogen bonds. In contrast, IR spectra are faster snapshots of the molecular motions; they are frozen and reveal that the situation is more complex.

As expected for dimers with little dissociation into monomers, the proton chemical shifts for the N-H functions of **1**−**4** in $CDCl_3$ are concentration independent over the range of concentrations studied. In contrast, the chemical shifts of **8** and **9**, which are unable to form stable spherical structures, distinctly change with concentration. For example, the NH resonances of **9** in $CDCl_3$ shift from 5.45 ppm at 1.5 mM to 6.17 ppm at 35 mM concentration. Aggregation through random hydrogen bonding is the likely cause for this downfield shift.

The ^{1}H chemical shifts of the NH resonances of self-complementary compounds **1**−**4** vary considerably with solvent. For example, in the NMR spectrum of **1·1** in $Cl_2DC-CDCl_2$, these signals appear 0.6 ppm downfield from their positions in CD_2Cl_2. The opposite effect is observed in the NMR spectra of **4**. Here, the NH signal is shifted upfield in $Cl_2DC-CDCl_2$ relative to spectra taken in CD_2Cl_2. In contrast, the appearance of NMR spectra of reference compounds **8** and **9** depends little on the solvent. In the following discussion, we present evidence that this solvent dependence is a consequence of host−guest interactions.

Encapsulation Experiments

As discussed earlier, dimerization of compounds **1**−**4** creates an internal cavity. It has been shown that the cavity of dimer **1·1** (and its phenylglycoluril analog) can be filled with guests of suitable size.[4] In some cases, detection of molecules contained inside the capsule of **1·1** was possible, For instance the ^{1}H NMR spectrum of **1·1** in $CDCl_3$ saturated with methane displays a strong singlet at −1.51 ppm.[15] Similarly, xenon was detected inside **1·1** by ^{129}Xe NMR.[4b] The encapsulation of other noble gases, as well as CD_2Cl_2 and even $CDCl_3$, was also reported.[4a] In these cases, however, the phenomenon was detected only indirectly.

In the presence of a large excess of the guest species (e.g., the solvent), a new set of signals appeared in the ^{1}H NMR spectrum, presumed to correspond to **1·1** with its cavity filled. For instance, when a solution of **1** in $CDCl_3$ (a guest too big to fit easily into **1·1**) was titrated with CD_2Cl_2, the appearance and growth of a new broad N-H signal in the ^{1}H NMR spectrum was observed at 8.5 ppm. This new signal arises from the dimer **1·1** containing CD_2Cl_2 in its cavity. The N-H proton appears shifted upfield by 0.6 ppm relative to "empty" **1·1**, the NH signals of which appear at 9.13 ppm. Presumably, this shift is due to elongation and weakening of the hydrogen bonds upon encapsulation of the guest. At 25 °C the signal for the "empty" dimer disappears completely as the concentration of CD_2Cl_2 in $CDCl_3$ reaches 20%. The ^{13}C NMR signal of CH_2Cl_2 *inside the cavity* of **1·1** has now been observed and confirms that. Upon addition of 10% by volume of $^{13}CH_2Cl_2$ (99% ^{13}C-enriched CH_2Cl_2) to a solution of **1** in $CDCl_3$ at 0 °C, a new signal, shifted 2 ppm upfield from free $^{13}CH_2Cl_2$, appeared in the ^{13}C NMR spectrum (Figure 3).[16] Its intensity relative to the ^{13}C NMR signals of the host dimer **1·1** (marked with △) suggests that the majority of host dimers contained labeled CH_2Cl_2 within their cavities. The experiment established that CD_2Cl_2 is a good guest for **1·1**.

Dimer **1·1** selects between methylene chloride and chloroform. Even at low temperature, $CDCl_3$ is not (or only very poorly) encapsulated by **1·1**. The question then remains, what is inside **1·1** when dissolved in a large solvent? Figure 4a shows the NH signal of **1·1** in $CDCl_3$ "from the shelf" at −20 °C. Clearly, several different species are present. If the sample is flushed with He, the appearance of the spectrum changes (Figure 4b) and only one broadened singlet 0.2 ppm downfield from the original multiplet can be found. Evidently, **1·1** encapsulates atmospheric gases, which can be removed by purging the sample with He. Unfortunately, it cannot be determined whether the NH resonance shown in Figure 4b corresponds to truly empty **1·1**, **1·1** containing helium, or a mixture of the two in rapid exchange.

The cavity of **2·2** is smaller than that of **1·1** and appears too small to accommodate CD_2Cl_2. This is probably why the chemical shifts of the N-H protons in CD_2Cl_2, $CDCl_3$, and $Cl_2DC-CDCl_2$ are all similar (Table 3). Nevertheless, dimer **2·2**

(15) For methane complexation inside a cryptophane, see: Garel, L.; Dutasta, J.-P.; Collet, A. *Angew. Chem., Int. Ed. Engl.* **1993**, *32*, 1169.

(16) This ^{13}C NMR technique has the advantage of eliminating overlapping signals as only enriched materials become visible.

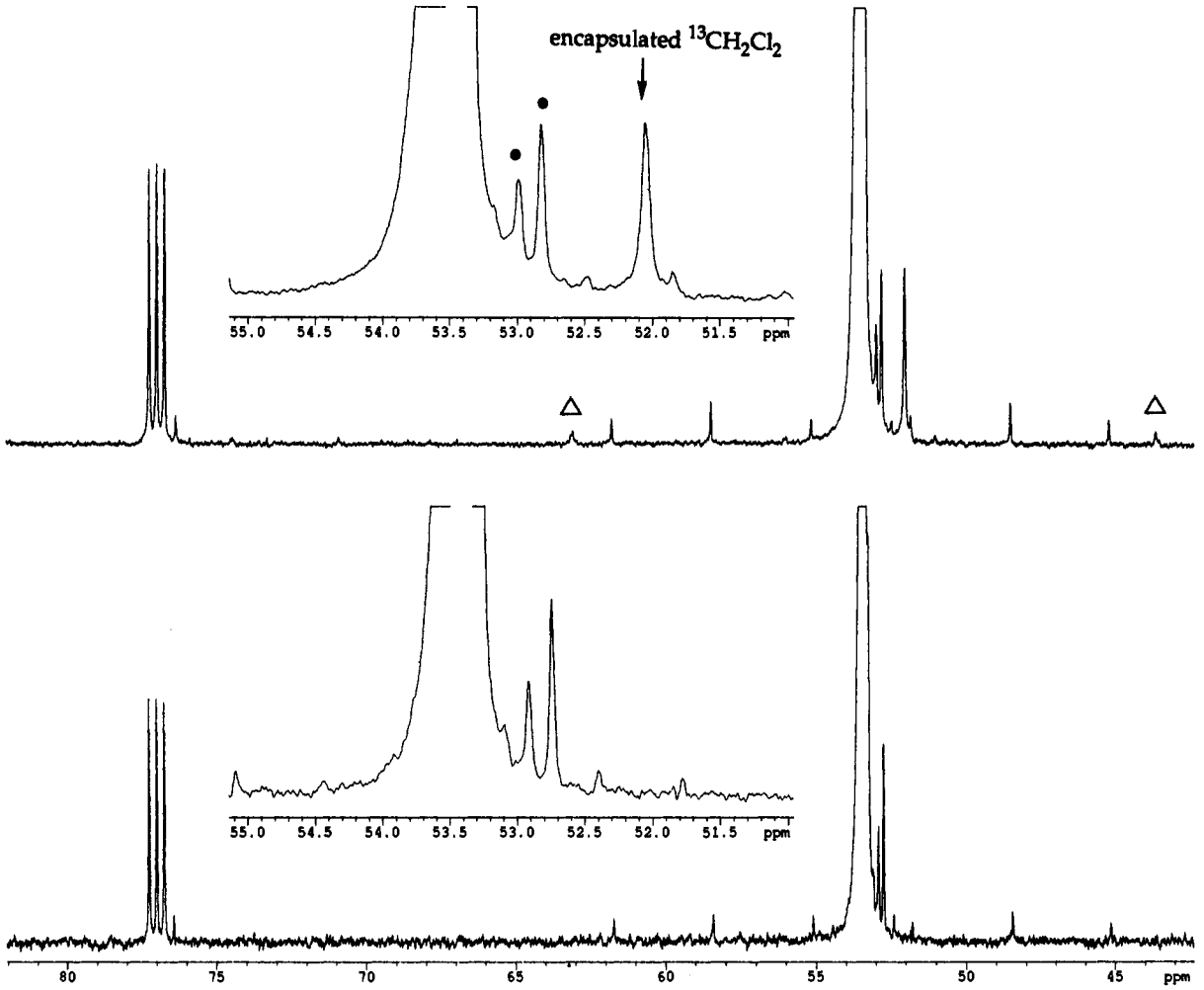

Figure 3. (top) ^{13}C NMR spectrum at 125 MHz of a 0.2 M solution of **1** in $CDCl_3$ containing 10% of $^{13}CH_2Cl_2$. The spectrum was taken at 273 K. (bottom) Solvent reference: ●, impurities in $^{13}CH_2Cl_2$; △, ^{13}C NMR signals of **1**.

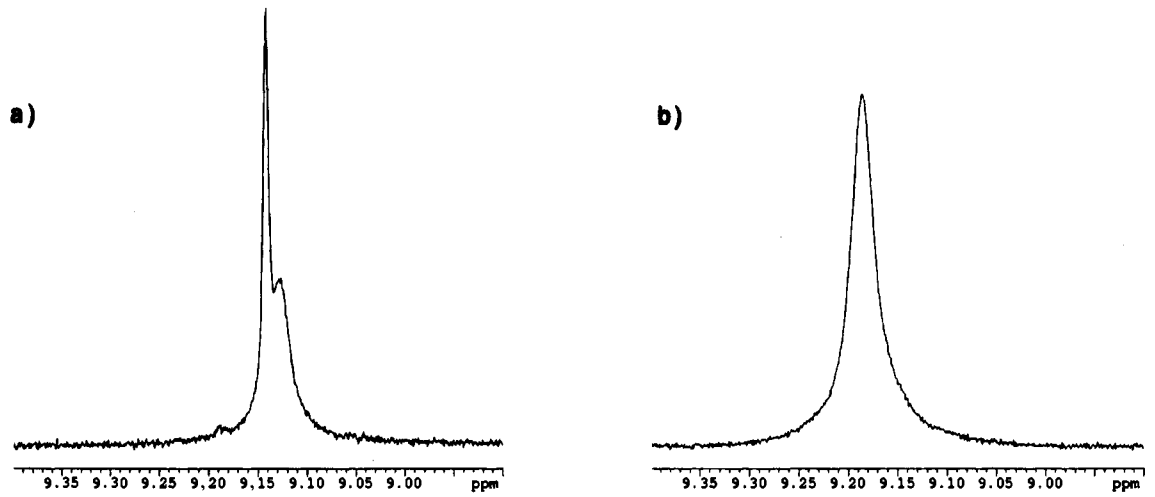

Figure 4. (a) ^1H NMR spectrum at 500 MHz of the NH region of **1·1** in $CDCl_3$ at −20 °C. (b) Identical spectrum after degassing the sample with helium.

can bind small molecules. Upon saturation of a $CDCl_3$ solution of **2·2** with methane, a new NH signal appeared in the ^1H NMR spectrum at 8.98 ppm in addition to the original one at 9,12 ppm. Besides the methane singlet at 0.22 ppm, a second singlet at −0.44 ppm appeared in the spectrum. In analogy to experiments with **1·1**, we assigned the upfield signal to methane inside the capsule. The affinity of methane for **2·2** is considerably less than for **1·1**; a binding constant $K^{273} = 4.2\ M^{-1}$ was measured for **2·2**, a value approximately 70 times lower than that found for the phenylglycoluril analog of **1·1**.[4a]

Nonetheless, dimer **2·2** displays a remarkable selectivity: ethane, which binds to **1·1** was not measurably encapsulated by **2·2**. From X-ray crystallographic data of the **1·1** and **2·2** dimers,[9] we calculate that the cavity formed by **2·2** (41 Å^3) is approximately 18% smaller than the one of **1·1** (50 Å^3) and is unable to accommodate the larger ethane.

Experiments with **4** also showed the consequences of its size and shape. For instance, when a solution of **4** in $Cl_2DC-CDCl_2$ (a poor guest for **4·4**) was titrated with $CDCl_3$ (a reasonably sized guest for **4·4**), the resonance for the NH signal gradually

Table 4. MM2-Minimized Dimers of Hybrid Dimers

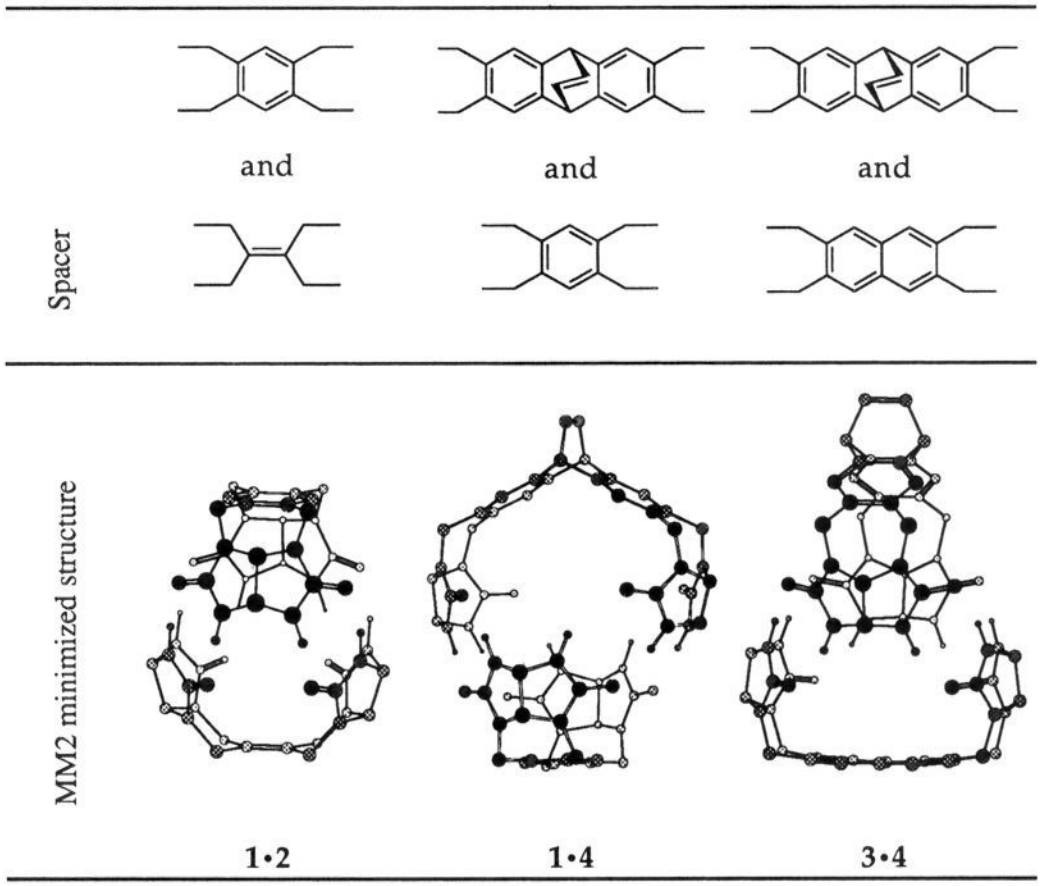

shifted. The NH signal moved downfield from 7.75 ppm and stabilized at 8.25 ppm after 20% $CDCl_3$ had been added. As $CDCl_3$ replaces the $Cl_2DC-CDCl_2$ from the cavity, a shortening and strengthening of the host's hydrogen bonds results. The rates of exchange processes with **4** were also different. Encapsulation experiments with the dimers **1·1** and **2·2** invariably showed two sets of ^1H NMR signals in the spectra, corresponding to slow exchange between the "empty" host and the host with its cavity filled.[3,4] However, this is not the case with **4.** Presumably, dynamic solvent exchange is fast on the NMR time scale, even at low temperatures.[17] As suggested by modeling studies, the openings of the dimer **4·4** are large enough for guest molecules to enter and escape the cavity either without breaking the host's hydrogen bonds or with breaking only a few of them (Table 1).

The case of **3·3** is also peculiar. The chemical shift of the NH protons in **3·3** strongly correlates with the size of the solvent used to record the NMR spectrum. The signal moves downfield with decreasing size of the solvent. Upon titration of a solution of **3** in $Cl_2DC-CDCl_2$ with CD_2Cl_2, the NH signal shifts gradually from 7.26 to 8.20 ppm. In 100% CD_2Cl_2 the signal appears at 8.28 ppm. This value is only 0.22 ppm upfield from that of **1·1** with CD_2Cl_2 encapsulated (a relatively stable complex). It appears that CD_2Cl_2 nucleates the formation of the dimeric **3·3** structure, although we were unable to provide more direct evidence. Molecular models suggest that, because the shape complementarity of the hydrogen binding sites in dimer **3·3** is poor, it can be stabilized by only four simultaneous hydrogen bonds. It is likely that the dimerization−dissociation processes involved in this case are fast, since a dimer with only four hydrogen bonds should be labile. At any rate, we were unable to find two separate sets of signals corresponding to "full" and "empty" **3·3**.

(17) The $Cl_2DC-CDCl_2$ solvent freezes at −40 °C and limits the temperature range for NMR experiments.

Formation of Hybrid Dimers

Structures **1**−**4** are designed to be self-complementary, and it is reasonable to expect that they also complement each other. Molecular models indicate that three combinations are especially suitable: hybrid structures **1·2**, **1·4**, and **3·4**.[18] The energy-minimized heterodimers are shown in Table 4.

Hybrid 1·2. The heterodimer **1·2** can be stabilized by eight hydrogen bonds comparable in geometry to those of the parent homodimers **1·1** and **2·2**. The ^1H NMR spectrum of a mixture of **1** and **2** in $CDCl_3$ did indeed show, besides the signals corresponding to **1·1** and **2·2**, a new set of signals. Since the two half shells of the hybrid are different, two new N-*H* resonances appeared, one at 8.71 ppm and the other at 9.33 ppm.

Since both dimers **1·1** and **2·2** were capable of binding methane in their internal cavities, it was reasonable to assume that the hybrid **1·2** would also make a good host for methane. Indeed, when a solution of **1** and **2** in $CDCl_3$ was saturated with methane, profound changes were observed in the NMR spectrum. Despite the complexity of the spectrum, we tentatively assigned the presence of six species: "full" and "empty" **1·1**, "full" and "empty" **2·2**, and "full" and "empty" **1·2**. Of special interest were the three different signals (Figure 5) corresponding to encapsulated CH_4: −1.51 ppm for CH_4 inside **1·1**, −0.44 ppm for CH_4 inside **2·2**, and −1.2 ppm for CH_4 inside **1·2**. As our methane source contained about 10% ethane, the signal for CH_3CH_3 inside **1·1** can also be observed.[4a] Again,

(18) For two-component assemblies based on calixarenes, see: Koh, K.; Araki, K.; Shinkai, S. *Tetrahedron Lett.* **1994**, *44*, 8255.

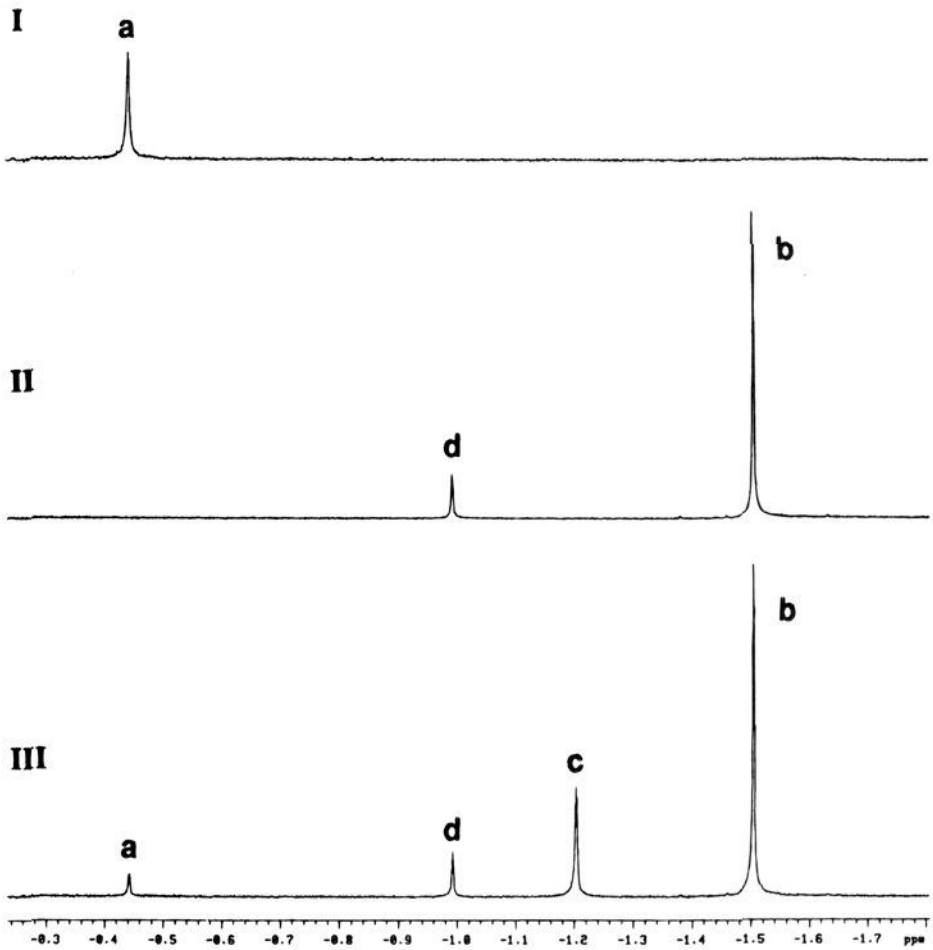

Figure 5. Partial ^{1}H NMR spectra at 500 MHz of a solution of **1** (II), **2** (I), and a mixture of **1** and **2** (III) in $CDCl_3$ saturated with methane. All spectra were recorded at 298 K. The labeled signals correspond to the resonances of CH_4 encapsulated by different species: (a) CH_4 inside **2·2**, (b) CH_4 inside **1·1**, (c) CH_4 inside **1·2**, and (d) CH_3CH_3 inside **1·1**.

the binding of methane occurs with some selectivity. There was no measurable encapsulation of ethane by **1·2**.

Hybrid 1·4. The geometry of the pear-shaped **1·4** allows the formation of only six "strong" hydrogen bonds. The ^{1}H NMR spectrum of an equimolar mixture of **1** and **4** in $CDCl_3$ showed signals corresponding to a new species, which we assigned to the heterodimer **1·4**. The "recombination" took place despite the inferior hydrogen bonding expected by modeling of **1·4**. This assignment was confirmed by NOE experiments. At −40 °C a strong NOE was observed in the heterodimer between the NH protons of the half-shells **1** and **4** when either of the glycoluril protons were irradiated (Figure 6).

As was the case with **4·4**, direct detection of guest molecules inside the cavities of **1·4** proved fruitless. The likely reason is that the openings of these capsules are large enough to permit rapid solvent exchange in and out of the cavities; the structure "leaks". The alternate explanation, rapid exchange between monomers and assemblies, is inconsistent with the observation of three discrete species in the NMR spectra.

Hybrid 3·4. Naphthalene derivative **3** failed to hybridize with **1** and **2**. Only poor hydrogen bonding is expected in **1·3** and **2·3**, whereas dimers **1·1** or **2·2** are well-bonded and would have to be disassembled in order to form hybrids. There is an entropic driving force, the reduction in symmetry (S_4 to C_{2v}) on mixing, but this appears to be insufficient to cause significant heterodimer formation in these cases.

Some new behavior emerged when solutions of **3** and **4** were studied by NMR in $CDCl_3$. In addition to signals corresponding to the homodimers, two new NH resonances were observed at 9.15 and 7.62 ppm. The energy-minimized structure for hybrid **3·4** predicts an aggregate similar to **1·4**. However, **3·4** is stabilized by only four short and two elongated hydrogen bonds. Despite the poor complementarity, the hybrid species is present in substantial amounts and even becomes the dominant species when occupied by a suitable solvent. This may be regarded as a solution-based nucleation phenomenon.

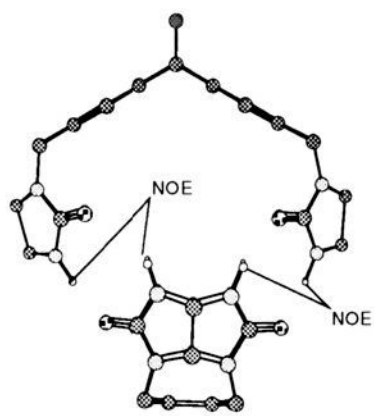

Figure 6. MM2-minimized structures of dimer **1·4.** Detected NOE effects are indicated.

Equilibrium Constants. The "recombination" of the homodimers to form hybrids is an equilibrium process. As the hydrogen bond arrays in the homodimers are generally superior to those of the heterodimers, the disproportionation must, to

Table 5. Equilibrium (Disproportionation) Constants, K,[a] for the Formation of Hybrids (Heterodimers) in Binary Mixtures using Solvents of Increasing Size, and Thermodynamic Values, ΔH and ΔS, for the Equilibrium in $CDCl_3$

$$K^{298} = \frac{[A{\cdot}B]^2}{[A{\cdot}A][B{\cdot}B]}$$

					ΔH (kcal/mol)	ΔS (eu)
hybrid dimer A·B	CD_2Cl_2	$CDCl_3$	$CDBr_3$	$CDCl_2CDCl_2$	$CDCl_3$	$CDCl_3$
1·2	0.08	0.9	0.7	0.9	2	8
1·4	no **1·4**	11.6	42	trace of **1·4**	−3	−5
3·4	0.2	5.7	62	0.6	5	21

[a] Determined by ^1H NMR by integration of the N−H signals of the different species (±10%).

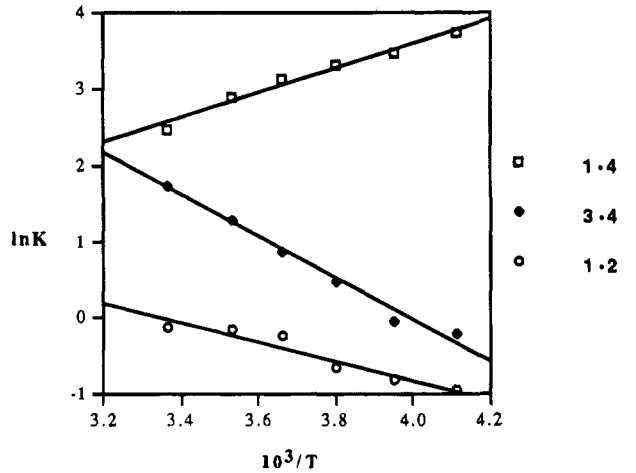

Figure 7. Plots of ln K (disproportionation constant) against $1/T$ (reciprocal temperature) for binary mixtures **1·2** (○), **1·4** (□), and **3·4** (◆) in $CDCl_3$ as obtained by VT NMR.

some extent, be entropically driven. We measured the disproportionation constants for the different hybrid capsules in solvents of varying size (Table 5) and over a concentration range. The distribution of species depended strongly on the solvent in which it was determined. Thermodynamic parameters for the disproportionation equilibria in $CDCl_3$ were deduced from variable-temperature ^1H NMR measurements (Table 5, Figure 7).

In the equilibrium of **1** and **2** with its hybrid, the disproportionation constant $K_{1\cdot2}$ (defined in Table 5) remains virtually constant in $CDCl_3$, $CDBr_3$, and $Cl_2DC-CDCl_2$ but is substantially smaller in CD_2Cl_2. Whereas the former three solvents are too large to fill the cavity of any of the three species present in the equilibrium, the latter (CD_2Cl_2) is of appropriate size to enter or, better, provide the driving force for the formation of **1·1**. For this reason the equilibrium distribution moves toward the homodimers in CD_2Cl_2; $K_{1\cdot2}$ decreases by about 10-fold from its value in the larger solvents.

Compounds **1** and **4** disproportionate in $CDCl_3$ exothermically, probably driven by tight binding of $CDCl_3$ in the hybrid, The extent of binding of $CDCl_3$ in the homodimer **4·4** (perhaps more than one $CDCl_3$ is involved) remains unknown. The cavity size of the three species **1·1**, **1·4**, and **4·4** obviously varies. As previously mentioned, the dimer of **1·1** readily encapsulates CH_2Cl_2 but not $CDCl_3$, whereas the bridged anthracene dimer **4·4** and the heterodimer **1·4** are both large enough to accommodate $CDCl_3$ and even $CDBr_3$. However, only **4·4** appears large enough to encapsulate $Cl_2DC-CDCl_2$. Accordingly the disproportionation constant increased from $CDCl_3$ ($K_{1\cdot4}$ = 11.6) to $CDBr_3$ ($K_{1\cdot4}$ = 42). Only traces of heterodimer **1·4** are formed in CD_2Cl_2 or $Cl_2DC-CDCl_2$. These results show that the "proper orientation" of hydrogen bonds is only part of the assembly story: although **1·1** enjoys hydrogen bonds of a more linear nature than those of **1·4**, the formation of the latter appears to be favored if its cavity is neatly filled.[19] It is worth emphasizing that the current state of predictions regarding the energetics and geometry of hydrogen bonds in such systems is far from ideal, and we hope that these studies will encourage research to place these inferences on firmer ground. Additional evidence for these nucleation effects in solution was provided by titration experiments. When a $CDBr_3$ solution of a mixture of **1** and **4** was titrated with CD_2Cl_2 (Figure 8, Table 5), the integration of the signals c and d corresponding to the heterodimer **1·4** decreased and resonance e at 8,25 ppm, corresponding to **1·1** filled with CD_2Cl_2, grew in.[20] Signal b, corresponding to homodimer **4·4**, increased stoichiometrically with that of **1·1** during the titration. The additional peak a in Figure 8 corresponds to empty **1·1**. The intensity of this signal decreases during titration as the cavity of **1·1** is filled (Table 6).[21]

The reverse process occurred when $CDCl_3$ was added to a solution of a mixture of **1** and **4** in $Cl_2DC-CDCl_2$ (Figure 9, Table 6). The concentration of **1·1** and **4·4** (signals a and b) decreased as the formation of **1·4** (signal d) became more and more pronounced (Figure 9, Table 6).

Solvent seems to also play a role in the formation of hybrid **3·4**. Its cavity size is similar to that of **1·4**, and the hybrid species is favored in $CDCl_3$ ($K_{3\cdot4}$ = 5.7) and $CDBr_3$ ($K_{3\cdot4}$ = 62!). Solvents CD_2Cl_2 and $Cl_2DC-CDCl_2$ are poor guest for the hybrid species; thus, no guest encapsulation assists the disproportionation and only small amounts of hybrid are formed in these solvents (Table 5).

A comparison of the thermodynamic parameters (ΔH and ΔS) determined for the disproportionation equilibria in $CDCl_3$ (Table 5, Figure 7) showed very different behavior for systems **1·2**, **1·4**, and **3·4**. The magnitude and the sign of the thermodynamic parameters for the **1·2** heterodimer are in agreement with what is expected from statistical distributions of dimers **1·1** and **2·2** in solution. In solvents which cannot fit inside, the value of the disproportionation constant is close to 1. The formation of **1·2** from homodimers **1·1** and **2·2** is expected to be an endothermic process (ΔH = 2 kcal/mol) since the hydrogen bonds in the homodimers appear superior to those in the heterodimer. The positive value for the entropy results from the loss of symmetry associated with the disproportionation process and the emergence of a new dissymmetrical hybrid species.

It is more difficult, however, to reconcile the magnitude and the sign of the thermodynamic parameters for hybrids **1·4** and **3·4** without quantitative knowledge of the number of species being encapsulated or released. Given the complexity of these

(19) Nucleation effects have also been observed in carceplexes and hemicarceplexes: (a) Cram, D. J.; Tanner, M. E.; Knobler, C. B. *J. Am. Chem. Soc.* **1991**, *113*, 7717. (b) Chapman, R. G.; Chopra, N.; Cochien, E. D.; Sherman, J. C. *J. Am. Chem. Soc.* **1994**, *116*, 369. (c) Chopra, N.; Sherman, J. C. *Supramol. Chem.* **1995**, *5*, 31.

(20) Titration of a solution of **1** in $CDBr_3$ with CD_2Cl_2 showed the same change in the chemical shift for the N-H proton.

(21) The NH resonance of **1·1** (Figure 5, signal a) displays a shoulder. This shoulder is most likely due to encapsulation of atmospheric gases, since it disappeared when the solution was purged with helium.

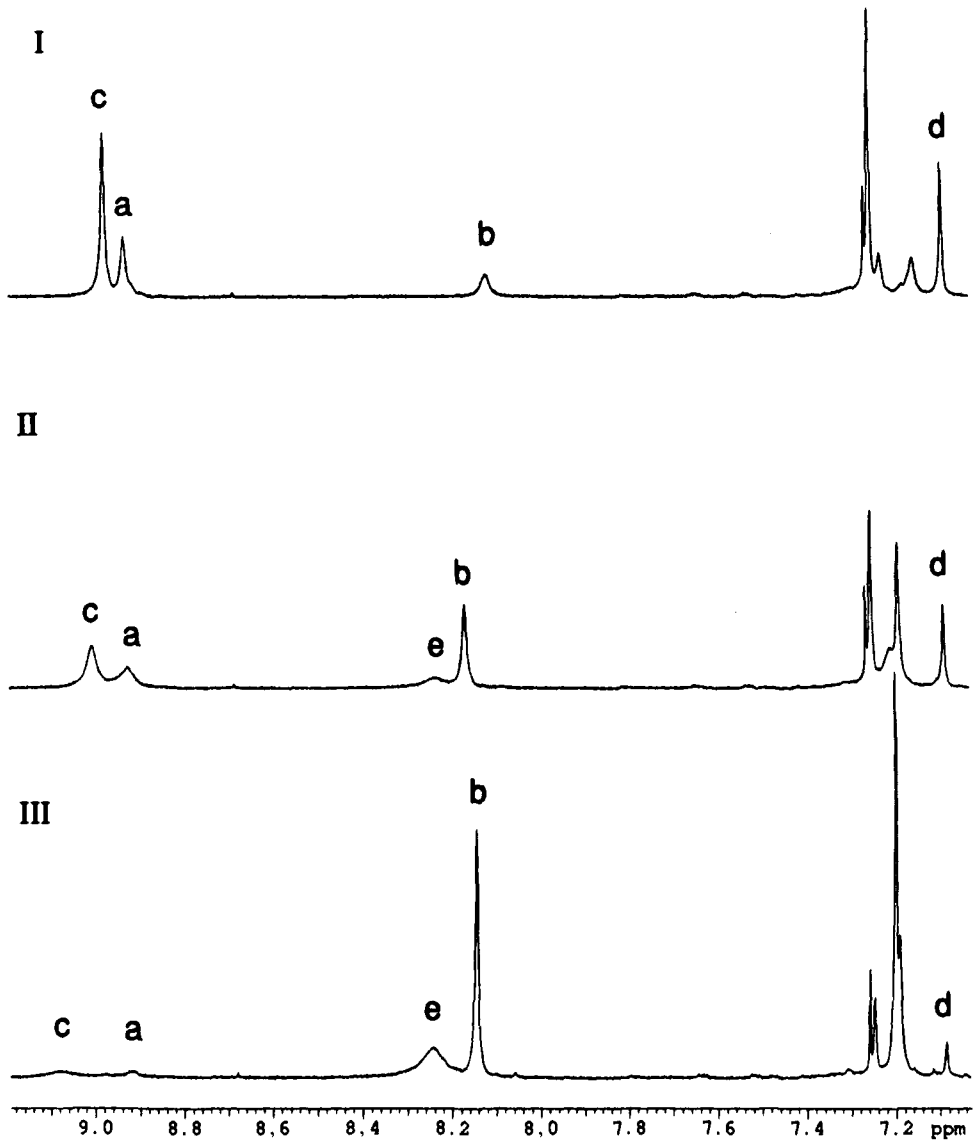

Figure 8. ^{1}H NMR (500 MHz) spectra (9.2−7.0 ppm) of the titration in $CDBr_3$ of a 1:1 mixture of **1** and **4**: (I) $CDBr_3$ solution; (II) $CDBr_3$ solution containing 5% of CD_2Cl_2; (III) $CDBr_3$ solution containing 18% of CD_2Cl_2. All spectra were recorded at 298 K. The labeled signals correspond to the resonances of the NH protons in the different species: (a) **1·1**, (b) **4·4**, (c) and (d) **1·4**, and (e) **1·1** with encapsulated CD_2Cl_2.

systems and our current knowledge of the different factors involved in the equilibrium processes, we are unable to perform a detailed analysis of this data; only a qualitative explanation, consistent with what has been observed above, can be proposed.

Conclusions

Direct evidence of the formation of capsular structures was obtained from the crystal structure of compound **1**, which was found to have the predicted dimeric structure **1·1** in the solid state as well as in solution. New monomers **2**, **3**, and **4** were synthesized and also shown to dimerize in nonpolar solvents. The resulting pseudo-spherical capsules feature internal cavities of varying sizes and shapes. These cavities can be filled with complementary guests, and we were able to observe directly guest molecules inside the capsules by NMR. Specifically, $^{13}CH_2Cl_2$ was detected inside **1·1** by means of ^{13}C NMR. The highly selective binding of methane in the presence of ethane by **2·2** was also observed. Indirect evidence for the encapsulation of solvent molecules of appropriate size by dimers **3·3** and **4·4** was deduced.

Formation of hybrid dimers **1·2**, **1·4**, and **3·4** was observed in solutions containing mixtures of two monomers. The disproportionation equilibria could be manipulated by the addition of appropriately sized solvents as guests. Even the energetically unlikely hybrids **1·4** and **3·4** were found to be the dominant species when suitable guests such as $CDBr_3$ were present. The existence of the heterodimers was confirmed by NOE measurements and through the selective encapsulation of methane.

Experimental Section

General Procedures. NMR spectra were recorded on Bruker AC250, Varian XL300, and Varian VXR 500 spectrometers with the solvents as the internal lock and internal references (^{1}H NMR: $CDCl_3$, 7.26 ppm; CD_2Cl_2, 5.32 ppm; $Cl_2DC-CDCl_2$, 5.90 ppm; $CDBr_3$, 6.82 ppm. ^{13}C NMR: $CDCl_3$, 77.0 ppm). Melting points were determined on a Thomas Hoover capillary apparatus and are uncorrected. Deuterated solvents and $^{13}CD_2Cl_2$ were purchased from Cambridge Isotope Labs. Anhydrous DMSO was obtained from Aldrich and used without further purification.

X-ray Diffraction Studies. A crystal of about 0.5 × 0.2 × 0.2 mm was mounted on a fiber embedded in a matrix of Paraton N. Data were collected at −66 °C on a Siemens CCD diffractometer (equipped with an automated three-circle goniometer and a solid state generator) using graphite-monochromatized Mo Kα (0.710 690 Å) by the ω scan

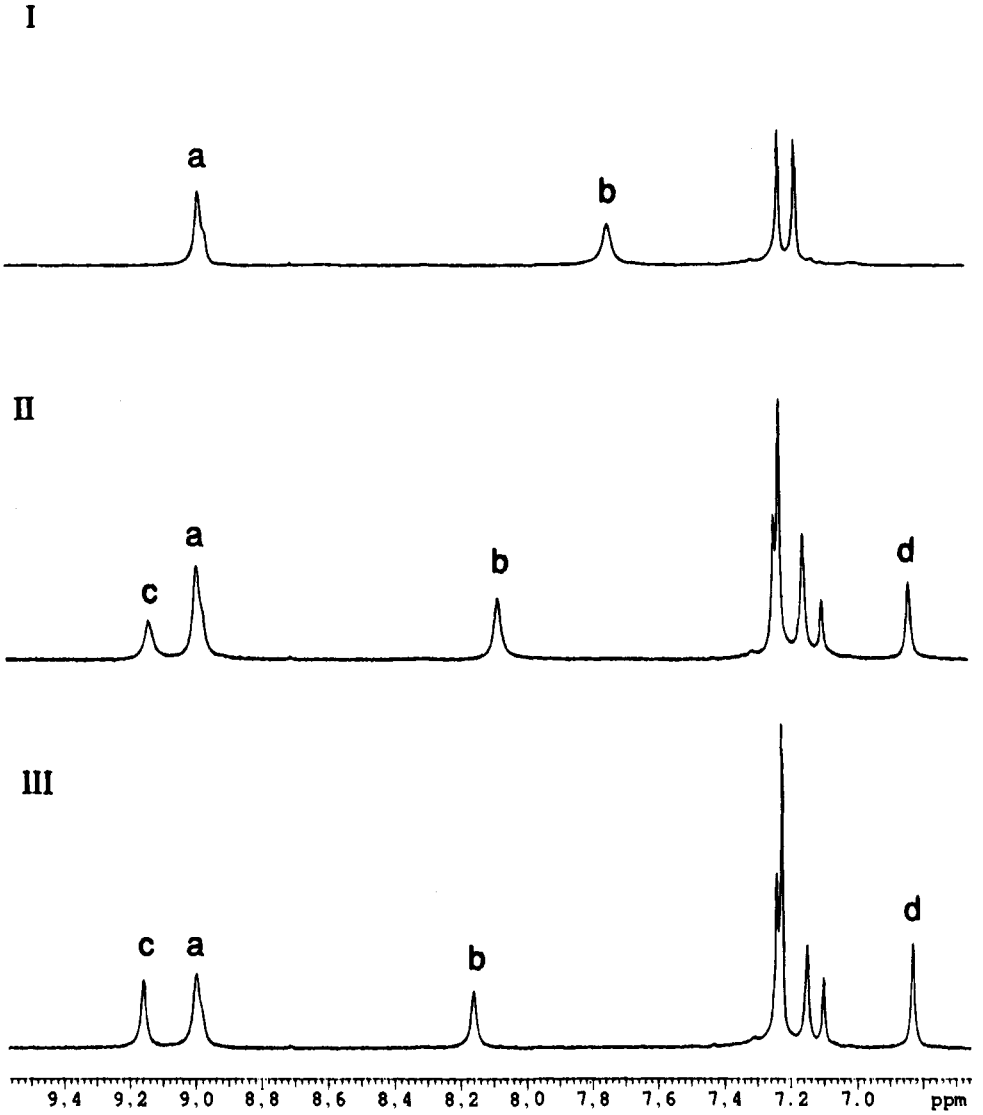

Figure 9. Titration of a 1:1 mixture of **1** and **4** in $Cl_2DC-CDCl_2$ with $CDCl_3$ monitored by ^1H NMR at 500 MHz: (I) no $CDCl_3$ added; (II) 10% of $CDCl_3$; (III) 15% of $CDCl_3$. All spectra were recorded at 298 K: (a) NH resonance of **1·1**; (b) NH resonance of **4·4**; (c and d) NH resonances of **1·4**.

Table 6. Equilibrium Concentration Changes in the Disproportionation of **1·1** and **4·4** on Titration with Different Guests

solvent	guest	favored species $\mathbf{1{\cdot}1} + \mathbf{4{\cdot}4} \rightleftharpoons 2(\mathbf{1{\cdot}4})$
$CDCl_3$	CD_2Cl_2	←
$CDBr_3$	CD_{2Cl2}	←
$Cl_2DC-CDCl_2$	$CDCl_3$, $CDBr_3$	→

method operating under the program SMART.[22] A total of 15 frames at 30 s measured at 0.3° increments of ω at three different values of 2θ and ϕ were collected, and after least squares, a preliminary unit cell was obtained. For data collection three sets of frames of 30 s exposure were collected. Data were collected in three distinct shells. For the first shell 606 frames were collected with values of $\phi = 0°$ and $\omega = -26°$, for the second shell 435 were collected with $\phi = 88°$ and $\omega = -21°$, and for the third shell values of $\phi = 180°$ and $\omega = -23°$ were used to collect 230 frames. At the end of data collection the first 50 frames of the first shell were recollected to correct for any crystal decay, but no anomalies were observed. The data were integrated using the program SAINT.[23] The integrated intensities of the three shells were merged into one reflection file. The data were filtered to reject outliers on the basis of the agreement of the intensity of the reflection and the average of the symmetry equivalents to which the reflection belongs. A total of 12 856 reflections were measured, ($2\theta_{max} = 46.6°$) of which 8853 were unique and 9038 had intensity above the $3\sigma(I)$ level. The R factor for averaged reflections was 0.062.

The space group is triclinic $P\bar{1}$ with unit cell dimensions $a = 13.924(3)$ Å, $b = 15.314(3)$ Å, $c = 18.094(4)$ Å, $\alpha = 92.09(3)°$, $\beta = 98.65(3)°$, $\gamma = 117.24(3)°$, and $V = 3366(2)$ Å^3 with $Z = 4$. The structure was solved using the direct methods program Sir92 of the TeXsan[24] crystallographic package of the Molecular Structure Corp. Full-matrix least-squares refinement with 4443 reflections ($2.7° < 2\theta > 40.9°$, $I > 3\sigma$) gave a final $R = 0.075$, $R_w = 0.074$. Missing atom positions were located from the difference maps calculated after several least-square cycles. All nonhydrogen atoms were refined anisotropically, except for carbonyl oxygens O5 and O7 which were disordered. This disorder was resolved, and O5 and O7 were refined at two positions each with 0.75/0.25 and 0.55/0.45 occupancies, respectively. Hydrogen atoms were located from the difference maps or placed in calculated positions. Only six hydrogens (N-*H*) were located from the difference maps; the rest were placed in calculated positions. The disorder inside the dimer could not be resolved, however; it was possible to refine the positions of a carbon atom with occupancies of 0.6/0.4.

Glycoluril Coupling Reactions. Bis(glycoluril) 2. Under an atmosphere of argon, ^{t}BuOK (3.3 g, 30.2 mmol) was added in one portion to 1,5-bis(carboxyethyl)glycoluril[4b] (4.5 g, 15.1 mmol) dissolved in dry DMSO (60 mL) at room temperature. After 15 min tetrakis-

(22) *SMART, V. 4.0*; Siemens Industrial Automation, Inc.: Madison, WI, 1994.

(23) *SAINT, V. 4.0*; Siemens Industrial Automation, Inc.: Madison, WI, 1995.

(24) *TeXsan Single Crystal Analysis Package, V. 1.7-1*; Molecular Structure Corp.: The Woodlands, TX, 1995.

(bromomethyl)ethene (**5**) (488 mg 1.22 mmol) was added. After being stirred for 60 min at room temperature, the mixture was poured into 0.1 N HCl (1 L). The resulting emulsion was extracted with ethyl acetate (3 × 400 mL). The combined extracts were washed with brine (3 × 300 mL), dried over Na_2SO_4, and evaporated to dryness, affording a white solid. The solid was stirred in chloroform (150 mL) for 30 min, and the resulting solution was filtered from the remaining solid. The filtrate was evaporated to dryness, furnishing essentially pure **2** (203 mg, 25%). The material was crystallized from $CHCl_3/CH_3OH$: mp 326 °C; ^1H NMR ($CDCl_3$) δ 9.06 (s, 4H, NH), 4.95 (d, 4H, J = 15.1 Hz), 4.23 (m, 8H, CH_2O), 4.49 (d, 4H, J = 15.1 Hz), 1.25 (m, 12H, CH_3) ppm; ^{13}C NMR ($CDCl_3$) δ 166.0, 165.6, 159.2, 122.9, 78.6, 74.9, 63.1, 63.0, 39.5, 13.9 ppm; HRMS calcd for $[M + H]^+$ 649.22180, found 649.21873.

Bis(glycoluril) 3, Tetrabromide **14** (400 mg, 0.8 mmol) was reacted with 1,5-bis(carboxybutyl)glycoluril[4b] (5 g, 14.7 mmol) as described above in the procedure for **2**. The reaction mixture was poured into 0.1 aqueous HCl (600 mL). The white solid which separated was collected by filtration and thoroughly washed with water and then dried. The resulting powder was stirred with chloroform for 2 h before the solution was filtered, and the filtrate was evaporated to dryness. Pure **3** (52 mg) was obtained after flash chromatography on silica gel, eluting with 5% CH_3OH in CH_2Cl_2: mp 308 °C; ^1H NMR ($CDCl_3$) δ 7.48 (s, 4H), 7.66 (s, 4H), 4.80 (d, 4H J = 15.5 Hz), 4.50 (d, 4H, J = 15.5 Hz), 4.24 (m, 8H), 1.8−1.4 (m, 16H), 1.03 (t, 6H J = 7.5 Hz), 0.99 (t, 6H J = 7.5 Hz) ppm; ^{13}C NMR ($CDCl_3$) δ 166.2, 165.8, 157.9, 133.8, 132.0, 129.0, 82.2, 74.6, 66.9, 66.8, 44.5, 30.4, 30.3, 19.1, 19.0, 13.8, 13.7 ppm; HRMS calcd for $C_{42}H_{52}N_8O_{12}$ $[M + H]^+$ 861.37829, found 861.37862.

Bis(glycoluril) 4, Glycoluril (0.68 g, 2 mmol) and ^{t}BuOK (0.45 g, 4 mmol) were reacted with tetrabromide **15** in dry DMSO (8 mL) as described above. The solid obtained from the reaction was stirred with chloroform (150 mL) for 30 min. The insoluble residue (consisting mainly of the undesired isomers) was removed by filtration. The filtrate was evaporated to dryness. The crude product solidified upon addition of ether. Column chromatography on silica gel eluting with 3%−7% CH_3OH in CH_2Cl_2 afforded the desired compound (12 mg, 12%): mp 302 °C; ^1H NMR ($CDCl_3$) δ 8.43 (s, 4H), 7.20 (s, 4H), 5.28 (s, 2H), 4.65 (d, 4H, J = 15.8 Hz), 4.35−4.15 (m, 16H), 1.50 (t, 6H J = 7.1 Hz), 1.26 (m, 12 H) ppm; ^{13}C NMR ($CDCl_3$) δ 165.9, 165.3, 164.8, 158.2, 143.3, 133.8, 129.0, 128.2, 82.0, 74.9, 62.9, 62.8, 61.5, 51.5, 43.9, 14.0 ppm; HRMS calcd for $C_{46}H_{48}N_8O_{16}$ $[M + H]^+$ 969.32665, found 969.32513.

Glycoluril 8, Compound **8** was synthesized following the procedure for **2**. Bis(carboxyethyl)glycoluril (2.1 g, 6 mmol) and ^{t}BuOK (1.3 g, 12 mmol) were reacted with 3-chloro-2-(chloromethyl)-1-propene (125 mg, 1 mmol) in 30 mL of dry DMSO. The white solid obtained from the reaction was washed with ether (50 mL) to give pure **8** (332 mg, 98%): mp 225 °C; ^1H NMR ($CDCl_3$) δ 6.29 (s, 2H, N-H), 5.04 (s, 2H), 4.42 (d, 2H, J = 15.1 Hz), 4.29 (m, 4H), 3.79 (d, 2H J = 15.1 Hz), 1.31 (m, 6H) ppm; ^{13}C NMR ($CDCl_3$) δ 165.9, 165.4, 157.2, 132.9, 114.5, 78.9, 73.6, 63.6, 63.2, 44.6, 14.0, 13.8 ppm; HRMS calcd for $[M + H]^+$ 338.12263, found 338.12180.

Glycoluril 9, The compound was obtained in the same way as described for **8**: α,α′-dichloro-*o*-xylene (175 mg, 1 mmol) was reacted to give **9** (325 mg, 84%) as a white solid: mp = 246 °C; ^1H NMR ($CDCl_3$) δ 7.4−7.2 (m, 4H), 5.83 (s, 2H, NH), 4.78 (d, 2H, J = 16.0 Hz), 4.44 (d, 2H, J = 16.0 Hz), 4.30 (m, 4H), 1.30 (m, 6H) ppm; ^{13}C NMR ($CDCl_3$) δ 166.0, 165.7, 157.0, 136.2, 129.6, 128.3, 83.2, 73.4, 63.6, 63.3, 44.8, 14.0, 13.8 ppm; HRMS calcd for $C_{18}H_{20}N_4O_6$ $[M + H]^+$ 388.138285, found 388.13881.

Synthesis of Tetrakis(bromomethyl) Compounds. 2,3,6,7-Tetrakis(acetoxymethyl)naphthalene, $LiAlH_4$, 1 M in THF (10 mL, 10 mmol), was added dropwise to a solution of tetracarboxylic ester **7** (300 mg, 0.828 mmol) in THF (20 mL) at room temperature. The mixture was stirred for 2 h, then a saturated aqueous solution of Na_2SO_4 was added dropwise with utmost care (!). The addition was continued until a solid separated and the supernatant became clear. The solvent was decanted, and the solid was washed with additional THF. Methanol (30 mL) was added to the remaining solid, and the mixture was heated to reflux for 3 h. After cooling, the methanol was decanted and the combined (CH_3OH and THF) solutions were dried (Na_2SO_4) and evaporated. The residue was dissolved in 10 mL of pyridine, and 1 mL of acetic anhydride was added. After stirring for 2 h all volatiles were removed *in vacuo*. The resulting solid was redissolved in ethyl acetate (25 mL), and the solution was washed with brine, dried over Na_2SO_4, and evaporated to dryness. Tetraacetate (235 mg, 68%) was obtained after flash chromatography on silica gel, eluting with hexane/ethyl acetate (1:1): mp 153 °C; ^1H NMR ($CDCl_3$) δ 7.85 (s, 4H), 5.31 (s, 8H), 2.11 (s, 12H) ppm; ^{13}C NMR ($CDCl_3$) δ 170.4, 132.8, 132.4, 128.8, 63.9, 20.8 ppm; HRMS calcd for $C_{22}H_{24}O_8$ $[M + H]^+$ 416.14653, found 416.14653.

2,3,6,7-Tetrakis(bromomethyl)naphthalene (6), A 30% solution of HBr in acetic acid (Aldrich, 5 mL) was added to tetraacetate (200 mg, 0.58 mmol) dissolved in 25 mL of chloroform. The mixture was stirred for 3 h and diluted with methylene chloride (30 mL). Saturated aqueous $NaHCO_3$ solution (30 mL) was added. The organic layer was separated, washed with brine, dried over Na_2SO_4, and evaporated to dryness. The crude product was obtained as a yellowish solid which was triturated with Et_2O to give the pure **6** (201 mg, 83%): ^1H NMR ($CDCl_3$) δ 7.82 (s, 4H), 4.82 (s, 8H) ppm; ^{13}C NMR ($CDCl_3$) δ 135.4, 133.2, 130.5, 30.4 ppm; HRMS calcd for $C_{14}H_{12}Br_4$ $[M + H]^+$ 259.012236, found 259.01225.

Bis(endoxide) 12a, A solution of 1,2,4,5-tetrabromobenzene (412 mg, 1.05 mmol) and of 2,3-bis(benzoxymethyl)furan (1.65 g, 5.28 mmol) in 50 mL of dry toluene was cooled to −23 °C under argon. BuLi (1.6 M in hexane, 2.31 mL) in dry hexanes (50 mL) was added dropwise over a period of 8 h. The mixture was stirred at −23 °C for an additional 8 h and warmed to room temperature, and then water was added. The aqueous layer was extracted with hexanes (2 × 30 mL). The combined organic layers were dried (Na_2SO_4) and evaporated to dryness. The oily residue was chromatographed on silica gel, eluting with hexanes/ethyl acetate (9:1 to 3:1). Early fractions contained unreacted furan which was recovered. Later, the two expected isomers eluted separately: the one eluting first being (most likely) the *anti* isomer.[11] *anti*-**12a** (207 mg, 15%): ^1H NMR ($CDCl_3$) δ 7.5−7.2 (m, 22H), 5.71 (s, 4H), 4.48 (d, 4H, J = 11.7 Hz), 4.33 (m, 8H), 4.10 (d, 4H, J = 12.8 Hz) ppm; ^{13}C NMR ($CDCl_3$) δ 148.3, 147.2, 137.6, 128.1, 127.4, 127.3, 112.9, 83.8, 71.7, 63.8 ppm. *syn*-**12a**: (168 mg, 12%): ^1H NMR ($CDCl_3$) δ 7.5−7.3 (m, 22H), 5.73 (s, 4H), 4.47 (d, 4H, J = 11.8 Hz), 4.38 (d, 4H, J = 11.8 Hz), 4.27 (d, 4H, J = 12.6 Hz), 4.03 (d, 4H, J = 12.6 Hz) ppm; ^{13}C NMR ($CDCl_3$) δ 148.3, 147.2, 137.6, 128.1, 127.4, 127.3, 112.9, 83.8, 71.7, 63.8 ppm; HRMS calcd for $C_{46}H_{42}O_6$ $[M + H]^+$ 691.30596, found 691.30488.

Tetrakis(benzoxymethyl)anthracene 13, Under an atmosphere of argon dry THF (10 mL) was slowly added to titanium(IV) chloride (0.48 mL, 4.38 mmol) cooled in an ice bath. $LiAlH_4$ (1 M in THF, 1.6 mL) was added, and the deep yellow suspension turned at first green, then black. Triethylamine (0.069 mL) was added, and the mixture was heated to reflux for 1 h. After cooling to room temperature, a solution containing **12a** (the mixture of the two isomers, 320 mg in 6 mL of THF) was added dropwise. After the mixture was stirred for 2 h, the reaction was quenched by addition of 20% aqueous K_2CO_3 (30 mL). The product was extracted with ethyl acetate (3 × 30 mL). The combined extracts were dried (Na_2SO_4) and evaporated to dryness to give the product as a yellow solid (315 mg, 99%) which was used without further purification: ^1H NMR ($CDCl_3$) δ 8.38 (s, 2H), 8.02 (s, 4H), 7.34 (m, 20H), 4.82 (s, 8H), 4.61 (s, 8H) ppm; ^{13}C NMR ($CDCl_3$) δ 138.0, 133.8, 131.0, 128.2, 127.6, 127.4, 125.6, 72.2, 70.0 ppm; HRMS calcd for $C_{46}H_{42}O_4$ $[M + H]^+$ 659.31613, found 659.31548.

Tetrakis(bromomethyl)anthracene 14, A solution of HBr (30% in AcOH, Aldrich, 10 mL) was added to a solution of tetrakis-(benzoxymethyl)anthracene (1.7 g, 2.58 mmol) in chloroform (70 mL). The resulting solution was stirred at room temperature for 2 h before the reaction was quenched with saturated, aqueous $NaHCO_3$. The mixture was extracted with CH_2Cl_2 (3 × 60 mL). The combined extracts were dried (Na_2SO_4) and evaporated to dryness. The residue crystallized upon trituration with ether. The pale yellow solid was recrystallized from ethanol to the desired tetrabromide (837 mg, 62%): ^1H NMR ($CDCl_3$) δ 8.33 (s, 2H), 8.02 (s, 4H), 4.92 (s, 8H) ppm; ^{13}C NMR ($CDCl_3$) δ 134.2, 131.9, 131.1, 126.8, 31.1 ppm; HRMS calcd for $C_{18}H_{14}Br_4$ $[M + H]^+$ 546.79072, found 546.78961.

Tetrabromide 15, A suspension of tetrakis(bromomethyl)anthracene (154 mg, 0.28 mmol) in a mixture of diglyme (3 mL) and diethyl acetylenedicarboxylate (1.5 mL) was refluxed for 60 min. The mixture was allowed to cool to room temperature, and the volatiles

were distilled *in vacuo*. The residue was chromatographed on silica gel, eluting with hexanes/ethyl acetate (9:1 to 3:1) to give the desired product (175 mg, 88%): ^{1}H NMR ($CDCl_3$) δ 7.39 (s, 4H), 5.46 (s, 2H), 4.57 (s, 8H), 4.24 (q, 4H, J = 7.0 Hz), 1.28 (t, 6H, J = 7.0 Hz) ppm; ^{13}C NMR ($CDCl_3$) δ 164.8, 145.6, 144.3, 134.4, 126.5, 126.2, 61.7, 51.4, 13.2 ppm; HRMS calcd for $C_{26}H_{24}Br_4O_4$ $[M + H]^+$ 716.84863, found 716.84782.

Acknowledgment. We are grateful to the National Institutes of Health for support. C.V. thanks the Ministerio de Educacion y Ciencia of Spain for a MEC Fulbright Fellowship, and U.P.S. thanks the Swiss National Science Foundation for a postdoctoral fellowship. We thank Dr. R. Aebi and E. A. Wintner for helpful discussions, Mr. Aaron L. Odun for help in crystal data collection, and Dr. William Davis for help in crystallography.

Supporting Information Available: A listing of crystallographic tables with bond lengths, bond angles, and positional and thermal parameters (27 pages). This material is contained in many libraries on microfiche, immediately follows this article in the microfilm version of the journal, can be ordered from ACS, and can be downloaded from the Internet; see any current masthead page for ordering information and Internet access instructions.

JA951886N